Photon-Photon Measurements in ATLAS

Chav Chhiv Chau on behalf of the ATLAS Collaboration
Carleton University, Ottawa, Canada

Abstract

At the Large Hadron Collider, two-photon production is a key process for studying photon interactions at high energies. Measurements of two-photon processes provide a direct access to the photon distribution function in protons and nuclei, and can probe the couplings between four vector bosons ($WW\gamma\gamma$) to find any deviation from the Standard Model. Two-photon measurements reported by the ATLAS Collaboration are presented. These measurements are performed using the proton-proton collisions at the centre-of-mass energy of 7 TeV ($pp \to pp\ell^+\ell^-$) and 8 TeV ($pp \to ppW^+W^- \to pp e^\pm\mu^\mp$), and using the lead-lead collisions at the centre-of-mass energy of 5.02 TeV (Pb + Pb $\to$ Pb + Pb + $\mu^+\mu^-$).

Keywords

Photon-photon production; exclusive dilepton; exclusive W boson pairs; QED; EWEAK; anomalous quartic gauge coupling

1 Introduction

Two-photon induced production is a purely electroweak process and has a relatively clean signature compared to most interactions recorded in the ATLAS experiment [1]. Indeed, the incoming protons or lead nuclei can create nearly-real photons coherently and escape the interaction with only a slight deviation with respect to their initial trajectories. Then, exclusive dileptons or W-boson pairs are produced via photon-photon scattering ($\gamma\gamma \to \ell^+\ell$, $\gamma\gamma \to W^+W^-$).

The ATLAS Collaboration has measured the exclusive production of dileptons ($pp \to pp\ell^+\ell^-$, where ℓ is an electron or a muon) and W-boson pairs ($pp \to ppW^+W^- \to pp e^\pm\mu^\mp$) in proton-proton ($pp$) collisions and exclusive dimuon production (Pb + Pb $\to$ Pb + Pb + $\mu^+\mu^-$) in lead-lead collisions. The measurements cover a wide range of the two-photon mass spectrum thanks to the LHC high centre-of-mass energy; for example, above the dilepton pair continuum of $m_{\mu\mu} = 10$ GeV for Pb + Pb $\to$ Pb + Pb + $\mu^+\mu^-$ production (a phase space not covered by previous measurements). They provide a way to determine the distribution of photons emitted from a proton and a nucleus. Furthermore, exclusive W^+W^- production is sensitive to the $WW\gamma\gamma$ quartic gauge couplings. The strength of the couplings can be extracted in order to compare to Standard Model prediction, since any deviation could indicate the existence of new physics.

The exclusive signal is modeled using the equivalent photon approximation (EPA) [2], which describes the fast moving proton and lead ion as structureless charged particle. As shown in Fig. 1, the proton scattering can be elastic where both protons remain intact, single-dissociative (SD) where one of them dissociates and double-dissociative (DD) where both fragment. The elastic process is characterized by the production of back-to-back leptons, i.e. the transverse momentum of the dilepton system $p_{\mathrm{T}}^{\ell\ell} \sim 0$, providing a way to separate the elastic from the dissociative production. For the heavy ion analysis, the dissociative interactions are not considered.

The following three measurements are presented here. The exclusive dilepton measurement [2] is performed using 4.6 fb^{-1} of pp collisions at the centre-of-mass energy of $\sqrt{s}$ = 7 TeV recorded in 2011. The exclusive W^+W^- analysis [3] is also performed with pp collisions, but using the dataset recorded in 2012 at $\sqrt{s}$ = 8 TeV corresponding to 20.2 fb^{-1}. Reported more recently, the Pb + Pb $\to$ Pb + Pb + $\mu^+\mu^-$ measurement [4] is done using a 515 μb^{-1} data sample collected at $\sqrt{s}$ = 5.02 TeV in 2015.

https://doi.org/10.23727/CERN-Proceedings-2018-001.45

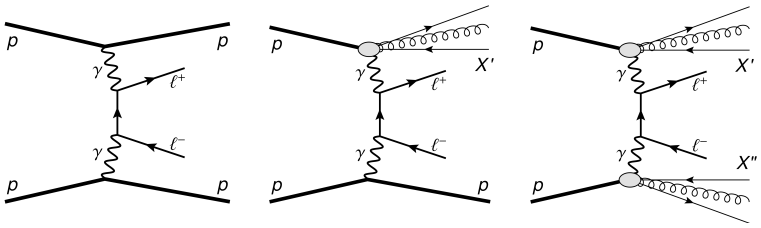

Fig. 1: Diagrams for the exclusive dilepton production representing the (left) elastic process, (centre) single-dissociation where one initial proton dissociates (SD) and (right) double-dissociation where both protons fragment (DD). The symbols X' and X'' denote any additional final state created.

2 Exclusive Dilepton Production

The exclusive dilepton analysis considers the e^+e^- and $\mu^+\mu^-$ final states. The data sample corresponds to 4.6 fb^{-1} of pp collision at $\sqrt{s}$ = 7 TeV recorded by the ATLAS experiment during 2011. The signal is the elastic dilepton production, while the single- and double-dissociative processes are considered as background. During the 2011 operation, many extra interactions occur during a same bunch crossing, so the signal events are selected only if they have a hard scattering vertex with exactly two lepton tracks isolated from other tracks and vertices.

2.1 Event Selection and Triggers

The events are first required to satisfy the following trigger logic: a muon with $p_{\mathrm{T}}^{\mu} > 18$ GeV or a dimuon with $p_{\mathrm{T}}^{\mu} > 10$ GeV for the muon channel; an electron with $p_{\mathrm{T}}^{e} > 20$ GeV or a di-electron with $p_{\mathrm{T}}^{e} > 12$ GeV for the electron channel. The exclusive events are selected by requiring a vertex with exactly two charged-particle tracks with $p_{\mathrm{T}}^{\mathrm{track}} > 0.4$ GeV and no extra tracks or vertices within a 3 mm longitudinal isolation distance from that dilepton vertex ($\Delta z_{\mathrm{Vtx}}^{\mathrm{iso}} > 3$ mm). Figure 2 illustrates the efficiency of the criteria in the muon channel. The exactly-two-tracks criterion suppresses Drell-Yan production and eliminates completely the diboson, multi-jet and top-quark backgrounds. The $\Delta z_{\mathrm{Vtx}}^{\mathrm{iso}} > 3$ mm requirement further suppresses Drell-Yan background, while retaining most of the signal. A large fraction of the Drell-Yan production that remains is rejected by vetoing the region 70 GeV $< m_{\ell^+\ell^-} <$ 105 GeV. Finally, a requirement on the dimuon transverse momentum $p_{\mathrm{T}}^{\ell^+\ell^-} < 1.5$ GeV is applied to reduce the dissociative background. This requirement suppresses single-dissociation by a factor of 3.

2.2 Measured cross section

At the LHC, the exclusive processes are suppressed due to the finite size of protons. The suppression is related directly to the probability of inelastic collisions [5] that rises with the centre-of-mass energy. The suppression factors are extracted from fits of the acoplanarity variable $(1 - |\Delta\phi_{\ell^+\ell^-}|/\pi$, where $\Delta\phi_{\ell^+\ell^-}$ is the azimuthal opening angle between the leptons.) An example of the fit is shown in Fig. 3 for the electron channel. As expected, the elastic dileptons have small acoplanarity compared to the single-dissociative events. The double-dissociative and Drell-Yan contamination is insignificant and is fixed to the Monte Carlo (MC) predictions. The acoplanarity fits estimate the elastic and SD fractions in data and determine the correction factors required to bring the simulation to agree with data. For the elastic signal, these factors are found to be $R^{\mathrm{excl}}_{\gamma\gamma\to e^+e^-} = 0.86 \pm 0.07$ and $R^{\mathrm{excl}}_{\gamma\gamma\to \mu^+\mu^-} = 0.70 \pm 0.04$ for the electron and muon channel, respectively. The SD factors are 0.76 for both channels.

The cross sections are measured in the fiducial regions defined by the following criteria: $p_{\mathrm{T}}^{e} > 12$ GeV, $|\eta^e| < 2.4$ and $m_{ee} > 24$ GeV for the electron channel; $p_{\mathrm{T}}^{\mu} > 10$ GeV, $|\eta^{\mu}| < 2.4$ and $m_{\mu\mu} > 20$ GeV for the muon channel. They are evaluated using the following relation:

$$\sigma^{\mathrm{excl}}_{\gamma\gamma\to\ell^+\ell^-} = R^{\mathrm{excl}}_{\gamma\gamma\to\ell^+\ell^-} \cdot \sigma^{\mathrm{EPA}}_{\gamma\gamma\to\ell^+\ell^-}, \quad (1)$$

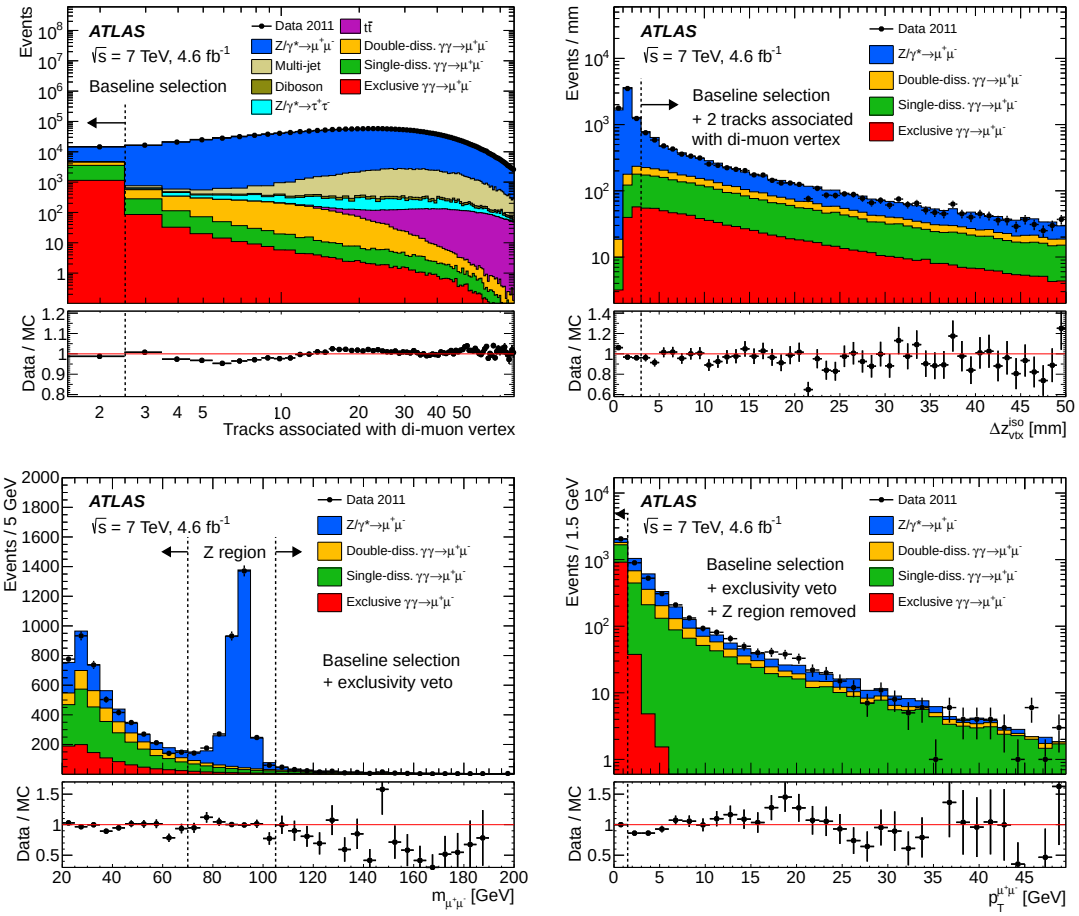

Fig. 2: The distributions of (top left) the number of tracks associated with the dimuon vertex, (top right) the longitudinal distance between the dimuon vertex and any other tracks or vertices, (bottom left) the invariant mass and (bottom right) the transverse momentum of the dimuon system. The black dashed lines and arrow indicate the requirements. More details can be found in Ref. [2]

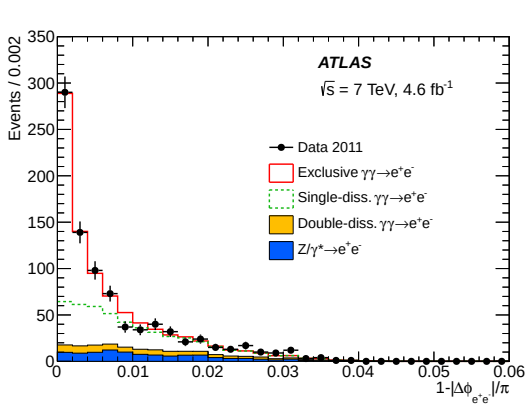

Fig. 3: Acoplanarity distribution of electron pairs passing all requirements. The elastic and SD yields are determined from the fit described in the text. More details can be found in Ref. [2].

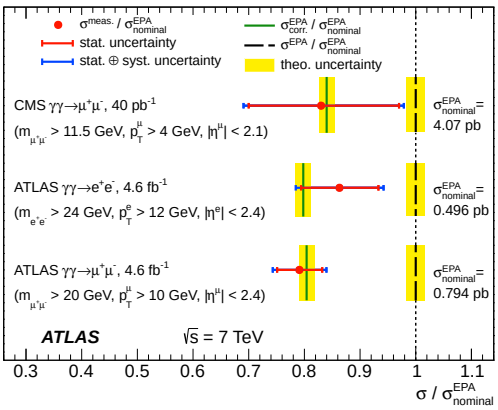

Fig. 4: Comparison of the ratios of measured (red points) and ratios of predicted (dashed line) cross section to the uncorrected EPA prediction [2]. A similar CMS measurement is also shown.

where $\sigma^{\mathrm{EPA}}_{\gamma\gamma\to\ell^+\ell^-}$ is the cross section calculated with the HERWIG++ generator [6] for the corresponding fiducial region.

The cross sections are determined to be 0.428 $\pm$ 0.035 (stat.) $\pm$ 0.018 (syst.) pb for the electron channel, and 0.628 $\pm$ 0.032 (stat.) $\pm$ 0.021 (syst.) pb for the muon channel. They agree within experimental uncertainties with the predictions [5]: 0.398 ± 0.007 (theor.) for the electron channel and 0.638 ± 0.011 (theor.) for the muon channel. More predictions [7] are available recently. Figure 4 shows the ratios of measured cross section to the prediction corrected for proton absorptive effects and to the uncorrected (nominal) prediction. A similar CMS measurement [8] is also included in the comparison. The measured cross sections are in agreement with the predicted values corrected for the proton absorptive effects [5].

3 Exclusive W^+W^- Production

The exclusive W^+W^- analysis considers the opposite-charge different-flavour $e^\pm\mu^\mp$ final states. The measurement is performed using 20.2 fb^{-1} of pp collisions at $\sqrt{s}$ = 8 TeV recorded by the ATLAS experiment during 2012. The exclusive W^+W^- process has a clean signature, since no extra activity is produced in addition to the two leptons. Also, it is a key process to probe the $WW\gamma\gamma$ quartic gauge couplings. Any enhancement of the coupling strength could indicate the existence of new physics.

Without tagging the initial state protons combined with having neutrinos in the final states, it is not possible to separate the elastic from the dissociative events. Therefore, the elastic, SD and DD W^+W^- processes are together considered as signal. The dissociative contribution is estimated from data, using an exclusive dimuon sample with $m_{\mu\mu} > 160$ GeV (twice the mass of W boson). The data-driven scale factor f_γ defined in Eq. (2) is given by the ratio of the number of data after subtracting off the number of background events ($\mathrm{N_{Observed}}$ - $\mathrm{N_{Background}}$) to the number of elastic events ($\mathrm{N_{Elastic}}$) predicted by HERWIG++. So the total expected signal for analysis is the prediction for the elastic W^+W^- production scaled by f_γ,

$$f_\gamma = \frac{\text{Elastic+SD+DD}}{\text{Elastic from MC}} = \left.\frac{\mathrm{N_{Observed}} - \mathrm{N_{Background}}}{\mathrm{N_{Elastic}}}\right|_{m_{\mu\mu}>160\text{ GeV}}. \tag{2}$$

3.1 Exclusivity Selection

The events selected for analysis satisfy any of the following triggers: a single-muon trigger with $p_{\mathrm{T}}^{\mu} > 24$ GeV, a single-electron trigger with $p_{\mathrm{T}}^{e} > 24$ GeV or an electron-muon trigger with $p_{\mathrm{T}}^{e} > 12$ GeV and $p_{\mathrm{T}}^{\mu} > 8$ GeV. The pileup conditions in 2012 are higher than in 2011. Therefore, a new track-based strategy for selecting exclusive events is developed for the analysis. The strategy starts by selecting two leptons with $p_{\mathrm{T}}^{\ell} > 20$ GeV and $m_{\ell\ell} > 20$ GeV. The event vertex is then reconstructed as the average of the longitudinal impact parameters (z_0) of the leptons: $(z_0^{\ell 1} + z_0^{\ell 2})/2$. Also, the two leptons are required to be within 1 mm in z of each other. At the next step, the longitudinal distance between the lepton vertex and other extra tracks (Δz_0) is computed. Finally, the exclusivity selection keeps only events with zero extra track within a 1 mm longitudinal distance of the lepton vertex ($\Delta z_0^{\mathrm{iso}}$ = 1 mm).

Cross-checks are done in the muon channel to validate the new strategy. Two of them are discussed here. The first cross-check extracts the suppression factor (f_{EL}) related to the proton absorptive effects and compares it to the expected value deduced from the exclusive dilepton measurement (Section 2.2). Similar fits of the acoplanarity variable are done, but with slightly different selection criteria: $p_{\mathrm{T}}^{\mu} > 20$ GeV, $m_{\mu\mu} > 45$ GeV, $|m_{\mu\mu} - m_Z| > 15$ GeV, $p_{\mathrm{T}}^{\mu\mu} < 3$ GeV and $\Delta z_0^{\mathrm{iso}}$ = 1 mm. The correction factor obtained is $f_{\mathrm{EL}} = 0.76 \pm 0.04(\mathrm{stat.}) \pm 0.10(\mathrm{syst.})$. Figure 5 shows the acoplanarity distributions of dimuons passing all the requirements. The elastic and dissociative contributions are corrected using the f_{EL} factor and the background is fixed to the Monte Carlo prediction.

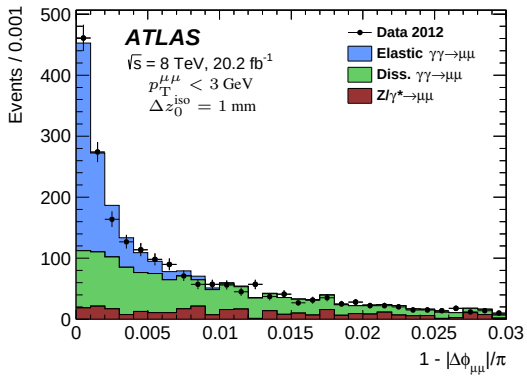

Fig. 5: Acoplanarity distribution of dimuons after requiring $p_T^{\mu\mu} < 3$ GeV and $\Delta z_0^{iso} = 1$ mm compared to data [3]. The elastic and dissociative yields are determined from the fit described in Section 2.2.

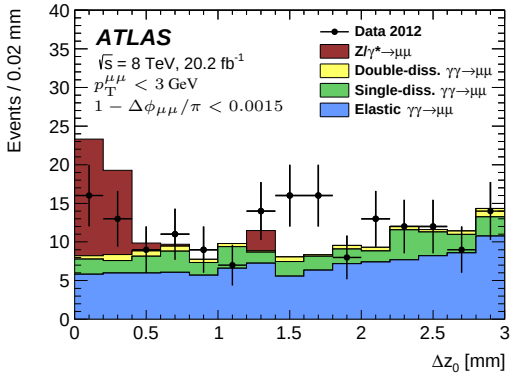

Fig. 6: Longitudinal distance between the lepton vertex and the closest extra track for dimuon events passing the criteria mentioned in the text [3].

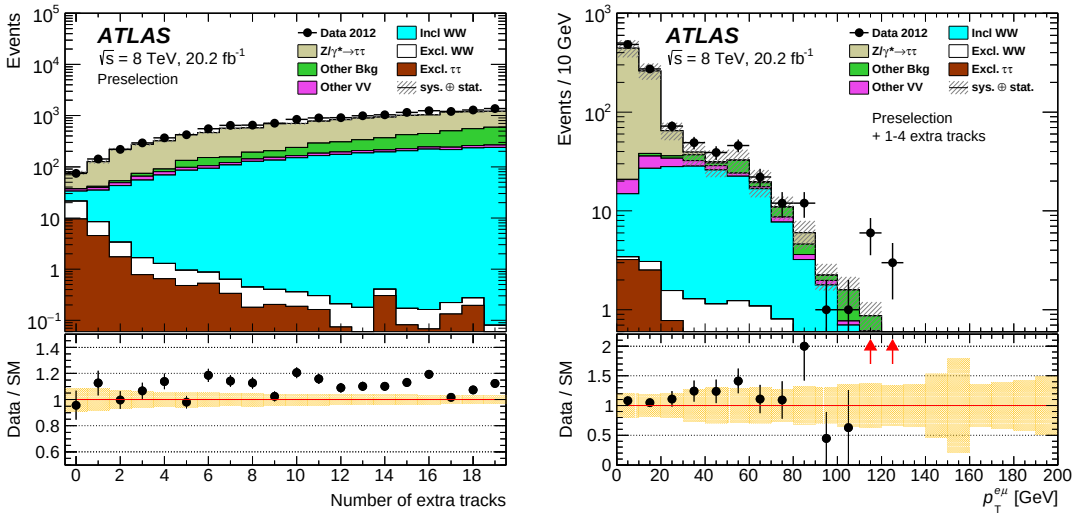

Fig. 7: Distribution of track multiplicities after requiring the exclusive W^+W^- preselection (Table 1) with no number of track dependent correction (left), and the $p_T^{e\mu}$ distribution of candidates that have 1–4 extra tracks (right). The enriched inclusive W^+W^- control region is the 1–4 extra-track region above $p_T^{e\mu} > 30$ GeV. The band around the Data/SM ratio of unity illustrates the systemic uncertainties. More details can be found in Ref. [3].

A second cross-check studies the pileup modelling and the effects of pileup on the efficiency of the exclusivity selection. Figure 6 compares the Δz_0 of simulated dimuon events to data. The events pass the same criteria as the previous cross-check, except that the acoplanarity < 0.0015 requirement replaces the exclusivity selection. The background passing all the criteria is Drell-Yan production and its Δz_0 distribution peaks at zero due to the underlying event (accompanying the hard interaction) producing extra tracks. For exclusive production, the extra track is a pileup track, so the Δz_0 distribution is flat.

3.2 Control Regions

Figure 7 shows the distribution of the number of extra tracks and the p_T spectrum of the events with 1 to 4 extra tracks. Selecting events with zero extra track keeps most of the signal, while eliminating a large fraction of background. Therefore, the events with 1–4 extra tracks constitute a good sample to control the background.

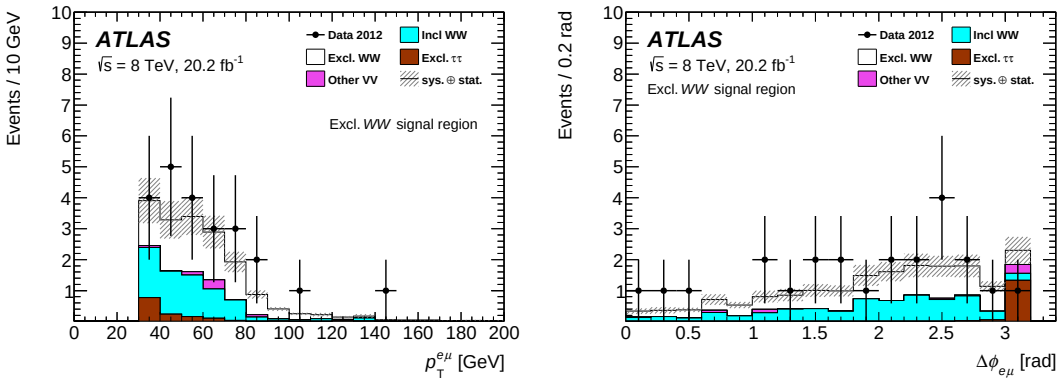

Fig. 8: Kinematic distributions in the exclusive W^+W^- signal region comparing the simulation to data [3].

3.3 Measurement

The event yields can be found in Table 1. The Preselection keeps good $e^{\pm}\mu^{\mp}$ events consistent with W-boson pair production. The $p_{\mathrm{T}}^{e\mu} > 30$ GeV requirement further reduce the Drell-Yan production and dissociative backgrounds. The exclusivity selection suppresses the inclusive W^+W^- background by three orders of magnitude. So, in the exclusive W^+W^- signal region, 23 candidates are observed in data, while 9.3 signal and 8.3 background events are expected. The observed significance over the background-only hypothesis is 3σ, constituting evidence of exclusive W^+W^- production in pp collisions. Figure 8 shows the $p_{\mathrm{T}}^{e\mu}$ and $\Delta\phi_{e\mu}$ distributions in the signal region. The simulation describes well the data.

The cross section times branching ratio is determined to be 6.9 ± 2.7 fb. It is consistent with the prediction. Since no significant excess over the Standard Model is observed, a 95% C.L. limit on anomalous quartic gauge couplings (aQGCs) is set.

	Signal	Data	Total Bkg	Incl WW	Excl. $\tau\tau$	non-WW	Other Bkg	MC/Data
Preselection	22.6 ± 1.9	99424	97877	11443	21.4	1385	85029	0.98
$p_{\mathrm{T}}^{e\mu} > 30$ GeV	17.6 ± 1.5	63329	63023	8072	4.30	896.3	54051	1.00
Exclusivity selection	9.3 ± 1.2	23	8.3 ± 2.6	6.6 ± 2.5	1.4 ± 0.3	0.3 ± 0.2	$---$	0.77
aQGC signal region								
$p_{\mathrm{T}}^{e\mu} > 120$ GeV	0.37 ± 0.04	1	0.37 ± 0.13	0.32 ± 0.12	0.05 ± 0.03	0	$---$	0.74

Table 1: The event yields at different stages of exclusive W^+W^- event selection [3]. The Preselection consists of the following requirements: exactly two $e^{\pm}\mu^{\mp}$ leptons, $p_{\mathrm{T}}^{\ell 1} > 25$ GeV, $p_{\mathrm{T}}^{\ell 2} > 20$ GeV and $m_{e\mu} > 20$ GeV.

The aQGC signal region has one additional requirement: $p_{\mathrm{T}}^{e\mu} > 120$ GeV. Figure 9 shows the $p_{\mathrm{T}}^{e\mu}$ of events passing all selection criteria apart for the one on $p_{\mathrm{T}}^{e\mu}$ itself. Several predictions for the aQGC parameters are shown as well, indicating that aQGCs would enhance the high $p_{\mathrm{T}}^{e\mu}$ region. The aQGC limits are evaluated using the one data candidate as constraint. The 95% confidence level contour and 1-dimensional limits are shown in Fig. 10. The limits obtained are consistent with the CMS combined 7 and 8 TeV measurement [9].

4 Dimuons in Lead-Lead Collisions

The heavy-ion measurement is of the cross section for exclusive dimuon production in lead nuclei collisions for invariant mass $m_{\mu\mu} > 10$ GeV. The data sample corresponds to 515 $\mu\mathrm{b}^{-1}$ of Pb+Pb collisions recorded by the ATLAS experiment in 2015. At high energy, the nuclei can produce quasi-real photons coherently with an enhancement of Z^2 over the incoherent production. In ultra-peripheral collisions, the two-photon production would be enhanced by Z^4. Therefore a significant rate of such QED processes is expected, although they have small cross section.

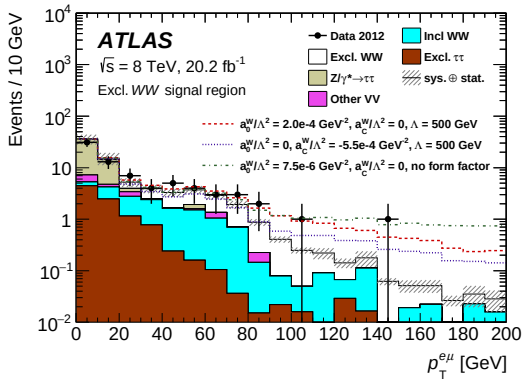

Fig. 9: Distribution of events passing all exclusive W^+W^- selection, except the requirement on $p_{\mathrm{T}}^{e\mu}$ [3]. Several aQGC scenarios are overlaid (dashed lines) as examples.

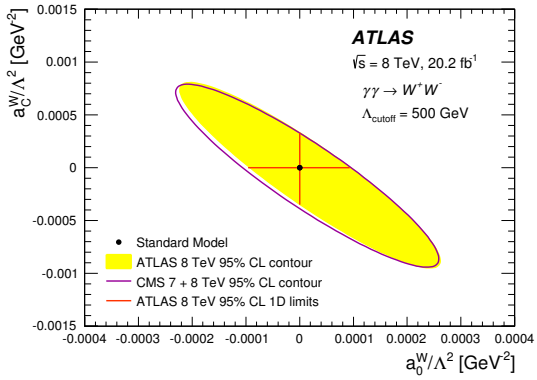

Fig. 10: The observed 95% confidence level contour and 1-dimensional limits [3]. The CMS combined 7 and 8 TeV result is shown for comparison.

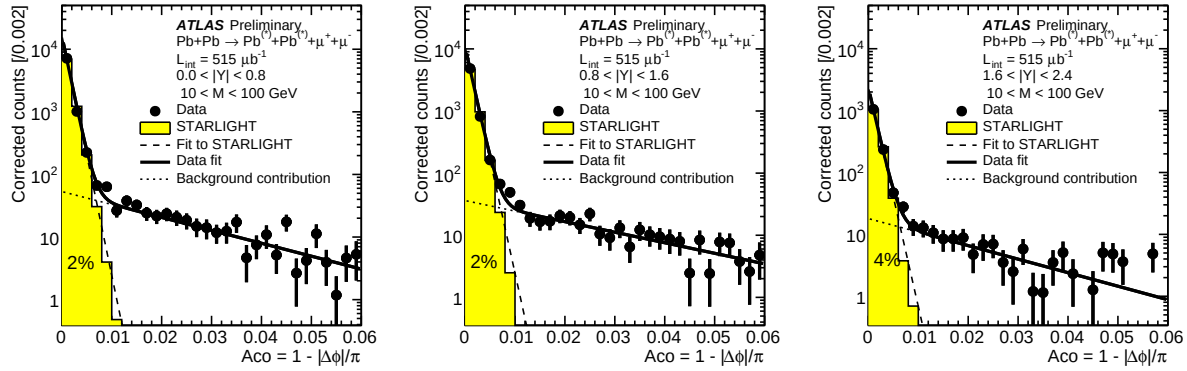

Fig. 11: Acoplanarity distributions for 10 GeV $< m_{\mu\mu} <$ 100 GeV in three dimuon rapidity bins: (left) $|Y_{\mu\mu}| <$ 0.8, (centre) $0.8 < |Y_{\mu\mu}| < 1.6$ and (right) $1.6 < |Y_{\mu\mu}| > 2.4$. More details can be found in Ref. [4].

4.1 Measurement

The events are selected if they have a muon and little additional activity in the detector. The selection of exclusive dimuons is similar to the dilepton analysis in pp collisions, i.e. events with a vertex with exactly two good opposite charged muons are selected. The signal is modelled using STARLIGHT [10]. For the run conditions of this analysis, it predicts kinematics coverage of dimuon mass up to 100 GeV.

Figure 11 shows the acoplanarity fits in the region 10 GeV $< m_{\mu\mu} <$ 100 GeV in three rapidity bins: $|Y_{\mu\mu}| < 0.8$, $0.8 < |Y_{\mu\mu}| < 1.6$ and $1.6 < |Y_{\mu\mu}| > 2.4$. Most signal events have very small acoplanarity, less than 0.008, as expected. Some activity is observed in the high acoplanarity tail. However, the composition of the events in the tail is unclear: it could be signal, background or a combination of the two. Therefore, two extreme cases are considered: all events in the high acoplanarity tail are signal; all of these events are background. The background estimate is then assumed to be the average of the two cases.

The cross section is determined in the following region: $p_{\mathrm{T}}^{\mu} > 4$ GeV, $|\eta^{\mu}| < 2.4$, $m_{\mu\mu} > 10$ GeV. The cross section for the fiducial region is $32.2 \pm 0.3(\mathrm{stat.})\,^{+4.0}_{-3.4}(\mathrm{syst.})\,\mu$b, consistent with the STARLIGHT prediction of $31.64 \pm 0.04(\mathrm{stat.})\,\mu$b. Figure 12 shows the cross section as function of $m_{\mu\mu}$ and $Y_{\mu\mu}$ for a few overlapping regions. The simulation describes the data well over the full kinematic range.

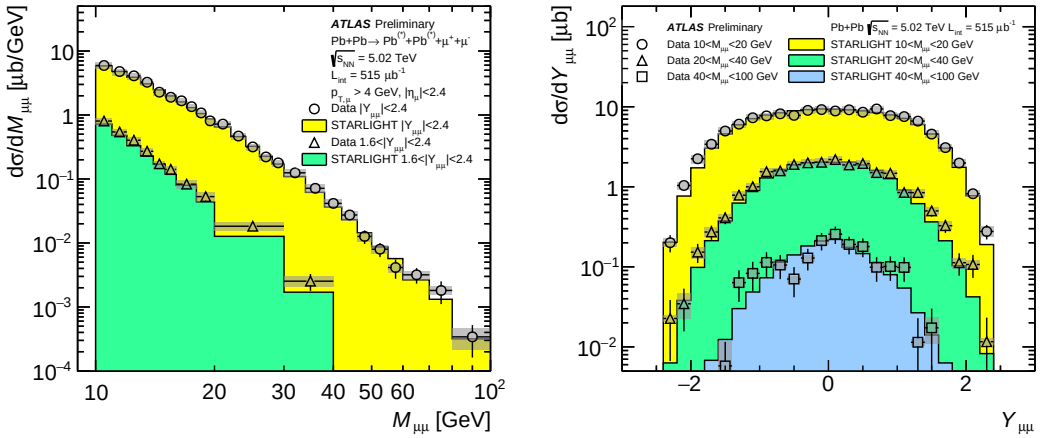

Fig. 12: Cross section for exclusive dimuon production in lead-lead collisions as a function of dimuon mass (left) and rapidity (right) [4]. Error bars indicate statistical uncertainties, while grey bands indicate the total systematic uncertainties.

5 Conclusion

Two-photon production of lepton pairs and W-boson pairs have been measured with the ATLAS detector. The proceedings present two measurements done using pp collision data, $pp \to pp\ell^+\ell^-$ at $\sqrt{s}$ = 7 TeV and $pp \to ppW^+W^- \to ppe^\pm\mu^\mp$ at $\sqrt{s}$ = 8 TeV, and a measurement of Pb + Pb $\to$ Pb + Pb + $\mu^+\mu^-$ production at $\sqrt{s}$ = 5.02 TeV. The ATLAS experiment has also reported 95% C.L. limits on the $WW\gamma\gamma$ anomalous quartic gauge couplings, extracted from the exclusive production of W-boson pairs. The measurements provide direct access to the elastic photon distributions in the proton and lead nucleus. Performed using a larger data sample compared to previous measurements resulting in an improved statistical precision, they provide a better understanding of photon interactions in hadron colliders.

References

[1] ATLAS Collaboration, JINST **3** (2008) S08003.

[2] ATLAS Collaboration, Phys. Lett. B **749** (2015) 242, arXiv:1506.07098 [hep-ex].

[3] ATLAS Collaboration, Phys. Rev. D **94** (2016) 032011, arXiv:1607.03745 [hep-ex].

[4] ATLAS Collaboration, ATLAS-CONF-2016-025, http://cds.cern.ch/record/2157689.

[5] Dyndal, M. and Schoeffel, L., Phys. Lett. B **741** (2015) 66, arXiv:1410.2983 [hep-ph].

[6] M. Bahr *et al.*, Eur. Phys. J. C **58** (2008) 639, arXiv:0803.0883 [hep-ph].

[7] L. A. Harland-Lang *et al.*, Eur. Phys. J. C **76** (2016) 9, arXiv:1508.02718 [hep-ph].

[8] CMS Collaboration, JHEP **01** (2012) 052, arXiv:1111.5536 [hep-ex].

[9] CMS Collaboration, JHEP **08** (2016) 119, arXiv:1604.04464 [hep-ex].

[10] S. R Klein *et al.*, Comput. Phys. Commun. **212** (2017) 258, arXiv:1607.03838 [hep-ph].